

# polymer papers

## A complete atomistic model of molten polyethylene from neutron scattering data: a new methodology for polymer structure

B. Rosi-Schwartz\* and G. R. Mitchell

Polymer Science Centre, J. J. Thomson Physical Laboratory, University of Reading, Reading, RG6 2AF, UK

(Received 25 January 1994; revised 24 May 1994)

A new approach to the study of the local organization in amorphous polymer materials is presented. The method couples neutron diffraction experiments that explore the structure on the spatial scale 1–20 Å with the reverse Monte Carlo fitting procedure to predict structures that accurately represent the experimental scattering results over the whole momentum transfer range explored. Molecular mechanics and molecular dynamics techniques are also used to produce atomistic models independently from any experimental input, thereby providing a test of the viability of the reverse Monte Carlo method in generating realistic models for amorphous polymeric systems. An analysis of the obtained models in terms of single chain properties and of orientational correlations between chain segments is presented. We show the viability of the method with data from molten polyethylene. The analysis derives a model with average C–C and C–H bond lengths of 1.55 Å and 1.1 Å respectively, average backbone valence angle of 112°, a torsional angle distribution characterized by a fraction of *trans* conformers of 0.67 and, finally, a weak interchain orientational correlation at around 4 Å.

(Keywords: polymer structure; molten polyethylene; neutron scattering)

### INTRODUCTION

The determination of the local organization of amorphous polymers remains to date a difficult and challenging endeavour. The application of techniques that have demonstrated a high level of success in explaining the structure of liquids composed of small rigid molecules is made rather difficult and unclear when the system of interest is composed of long molecules, characterized by conformational flexibility<sup>1,2</sup>. This is valid both from an experimental and a computational point of view. It is clear that even for molten polyethylene (PE), chemically the simplest polymer that is available, a great deal of discussion is still taking place in the literature, in an effort to establish the basis for analysis methods that will be suitable for more complex and more interesting polymeric materials.

Previous X-ray diffraction experiments<sup>3</sup> indicated the random coil nature of the PE chains in the melt, which were shown to be characterized by an irregular distribution of *trans* and *gauche* conformations, with about 40% *gauche* states, and which did not appear to exhibit extended conformations. These results confirmed earlier small angle neutron scattering<sup>4,5</sup> investigations, as well as theoretical predictions<sup>6</sup>. Similar conclusions were reached more recently by wide angle X-ray<sup>7,8</sup> and neutron<sup>9</sup> diffraction investigations. Furthermore, an interesting analysis of experimental data in terms of the recently developed polymer reference interaction site model (PRISM)<sup>10,11</sup> allows a calculation of the intrachain correlations to be performed; by subtracting this from

the total measured structure factor, a separation of the interchain contribution is then achieved<sup>8,12</sup>. The shortcomings of this approach arise from the indirect fashion by which important structural information is obtained. Different models for the polymer chain are simultaneously utilized on different chain length scales and Flory's 'ideality' postulate<sup>13</sup> has to be invoked to ensure the independence of intra and interchain correlations.

In the modelling realm the situation is somewhat similar. In recent years there has been a great deal of interest in applying atomistic simulation techniques to obtain models of macromolecules using both Monte Carlo<sup>14,15</sup> and molecular dynamics<sup>16,17</sup> approaches. However, due to the enormous range of lengths and time scales that need to be accessed in such systems, the task has been demonstrated not to be easy and straightforward. The convergence of these simulation algorithms has been achieved at the expense of a realistic treatment of the macromolecules at the level of the chemical structure. Rather crude and simplified treatments of the intra and intermolecular interactions have been put forward, in which groups of successive chemical monomers have been taken together to form effective segments, in a 'coarse grain' approach, thereby averaging out all interesting information at the molecular level. Only recently has attention shifted towards simulations of small groups of monomers<sup>18–20</sup>. These investigations access structural information on the spatial scale of the persistence length of the chain. In the case of PE, the models thus obtained are successful in predicting a number of properties but are still unrealistic on the chemical bond length scale.

\* To whom correspondence should be addressed

In this paper we report a new study of molten PE, which couples experimental neutron diffraction over a wide momentum transfer range with modelling techniques. Starting from an initial polymer configuration, we have used the reverse Monte Carlo (RMC) approach to obtain a structural representation of PE *exclusively* from experimental information. The realistic character of the obtained model has been determined by an analysis of both its single chain and its bulk properties, which are consistent with results in the literature, when available. We have also explored the possible existence of interchain orientational correlations, previously predicted theoretically but never observed experimentally. On the other hand, we have compared this modelling strategy with dense PE structures generated by entirely different atomistic modelling techniques, namely molecular mechanics and molecular dynamics, which are totally independent from experimental data. The structures provided by the two different routes are characterized by very similar properties and represent with equal accuracy the experimental results over all length scales. In essence we have validated the force field used in the molecular dynamics procedure to generate these structures. We have thus achieved the twofold purpose of showing the viability of RMC as a tool for the structural investigation of amorphous polymers and of obtaining, we believe for the first time, a complete model for molten PE.

## NEUTRON DIFFRACTION THEORY

Thermal neutrons can exchange both energy and momentum with the system in study, due to their wavelength and energy characteristics. However, if the incoming neutron energy is large compared to the typical values of energy exchange with the system, the collision can be considered elastic, and hence  $|k_f| = |k_i|$ , where  $k_i$  and  $k_f$  are the wave vectors characterizing the incident and scattered neutron respectively. This constitutes the so-called static approximation.

The amplitude of the momentum transfer  $Q = k_f - k_i$  is then given by the relationship  $Q = 4\pi \sin \theta / \lambda$ ,  $2\theta$  being the scattering angle and  $\lambda$  the incident neutron wavelength.

The measured intensity is proportional to the differential scattering cross-section, which in turn can be related to the static structure factor  $S(Q)$  characterizing the system. In the simple case of a disordered system composed of  $N$  identical nuclei, the differential scattering cross-section is given by the following relationship:

$$\frac{d\sigma}{d\Omega} = Nb^2 S(Q) \quad (1)$$

where  $b$  is the scattering amplitude of the identical nuclei.  $S(Q)$  is defined as the spatial Fourier transform of the atomic pairwise correlations functions:

$$S(Q) = 1 + \rho_0 \int_0^\infty [g(r) - 1] e^{iQr} dr \quad (2)$$

where  $\rho_0$  is the average density of the system and  $g(r)$  is the pair distribution function, expressing the probability that there exists an atom at a distance  $r$  from the origin atom. The radial distribution function and, similarly,  $S(Q)$  are split into partial terms for systems containing more than one chemical species.

The structure factor  $S(Q)$  is readily determined from

the experiment (equation (1)), while a model structure factor can be easily derived (equation (2)) if the coordinates of the atoms within the model are known. Hence one approach to structural analysis is to devise an algorithm for the generation of atomistic models which are quantitatively evaluated by comparison of their calculated structure factor with the experimentally derived  $S(Q)$ . This approach forms the basis of the present work.

## EXPERIMENTAL

The deuterated linear PE was obtained from MSD Isotopes, Canada. The deuteration level was 99%; a g.p.c. measurement gave average molecular weights  $M_w = 205\,000$  and  $M_n = 58\,000$ , with a polydispersity equal to 3.5. The material was sintered at room temperature to produce a flat pellet of thickness 0.8 mm. The specimen was contained in a heated TiZr can; the temperature of the sample was homogeneous within 1°C.

The experiment was performed on the novel time-of-flight diffractometer SANDALS at the ISIS facility (Rutherford Laboratory, Chilton, UK), whose principle of operation is described in detail elsewhere<sup>21</sup>. The usefulness of this diffractometer for the study of the local structure in polymeric materials has been outlined elsewhere<sup>22</sup>. Measurements, performed in high vacuum at 145°C, lasted about 10 h. The sample was checked after the measurements and it did not show any signs of oxidation or degradation. The diffractometer provided information over a broad and continuous momentum transfer range,  $Q \approx 0.2 - 50 \text{ \AA}^{-1}$ . In order to test the reproducibility of the instrument, measurements were performed in successive 2 h runs which were individually checked and compared with each other before being summed together.

For each one of the 10 detector banks, the raw data were normalized for the incident beam flux and calibrated with a standard flat plate vanadium sample. Corrections were made for absorption, multiple scattering and self-scattering contributions. Data from the different detector banks were finally merged together and the total structure factor  $S(Q)$  was obtained. This data reduction was performed with the ATLAS suite of programs available at ISIS for the analysis of time-of-flight diffraction data<sup>23</sup>.

## GENERATION OF ATOMIC COORDINATES FOR THE INITIAL MODEL

The starting three-dimensional model for PE was generated with a commercial materials simulation package, Quanta by Molecular Simulations Inc. The calculations were performed on a Silicon Graphics 4D/35 workstation.

Bulk PE specimens were created by growing a single PE chain in a unit cell, subject to periodic boundary conditions. A 700 CH<sub>2</sub> monomers chain was grown in an amorphous structure in a cubic box, whose dimensions were determined by the required bulk density. We grew our samples at the real bulk density of PE, i.e. 0.85 g cm<sup>-3</sup>. This corresponded to a cell dimension of 27.67 Å.

The amorphous growth algorithm employed was very similar to that previously reported in the literature by Fan *et al.*<sup>24,25</sup>. The polymer is generated by placing one

repeat unit, or residue, at a time, until the complete chain is packed in the cell. The placement of each residue is governed by the energy of the system: the conformation resulting from the addition of the new residue is accepted or rejected based upon one of a few possible energy selection criteria. The process could be viewed as one in which the unit cell is surrounded by periodic images of itself; once the chain reaches a cell boundary, it becomes truncated and its mirror image starts growing on the opposite side of the cell.

In more detail, torsion angles are assigned values by random sampling, according to a rotational isomeric state (RIS) model, representing the equilibrium conformational states of the polymer. The RIS model is only used as a convenient strategy to build chains in very different conformations depending upon the statistical weights assigned to the torsional angles. Thus the configurational space is widely explored in terms of the population of rotational states and its distribution. By using this method, we built several models characterized by very different initial conformations; however, such structural differences disappeared once we subjected the amorphous samples to relaxation procedures yielding equilibrated structures, as will be shown later.

The energy added through the placement of each residue is then computed. This energy considers all interactions of the residue with respect to itself and to the periodic images of all previously placed residues. The minimum image convention chooses atom pairs with the lowest separation; only non-bonded interactions within a specified cutoff distance are considered. In our case the value chosen for this distance was 14 Å; this value was estimated from the breadth of the main interchain peak measured at  $1.3 \text{ \AA}^{-1}$  in previous X-ray diffraction experiments. Since the minimum distance allowed for two non-bonded atoms is the sum of the van der Waals radii of the atoms, the growth process is extremely facilitated if the van der Waals radii of all atoms are reduced by a common factor. We used van der Waals radii that were 70% of their real values.

It should be noted in this respect that an alternative common trick to facilitate the growth process consists in the elimination of all hydrogen atoms in the structure. Since we were interested in a model that could predict all the possible local structural correlations present in the experimental diffraction pattern, we decided not to follow this route; we built a complete PE chain, inclusive of its hydrogen atoms.

Once the energy of the newly added residue is computed, a selection criterion is applied to determine whether or not the conformation is acceptable. Although in our case several models were built corresponding to different selection criteria, the resulting structures did not seem to depend crucially on the chosen criterion. The results that we will present here correspond to a Boltzmann selection approach. This implements the Metropolis algorithm: if the new conformation is of lower energy, then it is selected; if it is of higher energy, it is accepted with probability equal to the Boltzmann factor  $\exp(-\Delta E/k_B T)$ , where  $T$  is the temperature of the system,  $k_B$  is the Boltzmann constant and  $\Delta E$  is the energy difference between current and previous conformations. If the conformation is rejected, the random placing process is continued until the new conformation is accepted or a specified maximum number of trials (in our

case 50) has been reached. In this last, case, the previous residue is erased and randomly placed again, according to a procedure called 'backtracking'.

For each chosen growth strategy, we generated five structures in order to obtain suitable statistics for the ensuing analysis. The structure generated by the described procedure is in a high energy state, and therefore unrealistic, mainly due to the steric interactions related to non-bonded van der Waals forces.

## REVERSE MONTE CARLO TECHNIQUE

The dense PE model obtained with the technique described in the previous section was used as starting configuration in an RMC calculation<sup>26</sup>. The basic idea of this method is the modification of the initial three-dimensional configuration of the system to fit experimental diffraction data, following an algorithm that is a variation of the standard Monte Carlo procedure. We will summarize the salient points of the method, which is described in detail elsewhere<sup>27</sup>.

Given a starting configuration, if  $S^E(Q_i)$  and  $S^C(Q_i)$  are the experimentally measured and calculated structure factors respectively, the difference between them is:

$$e_i = S^E(Q_i) - S^C(Q_i) \quad (3)$$

which has a probability:

$$p(e_i) = \frac{1}{\sqrt{2\pi}\sigma(Q_i)} e^{-e_i^2/2\sigma^2(Q_i)} \quad (4)$$

where  $\sigma(Q_i)$  is the standard deviation of the normal distribution. The corresponding total probability for all the  $Q_i$  points is:

$$P = \prod_{i=1}^{m_Q} p(e_i) = \left( \frac{1}{\sqrt{2\pi}\bar{\sigma}} \right)^{m_Q} e^{-\sum_{i=1}^{m_Q} e_i^2/2\sigma^2(Q_i)} \quad (5)$$

where  $m_Q$  is the number of  $Q_i$  points in  $S^E$  and it is:

$$\bar{\sigma} = \left[ \prod_{i=1}^{m_Q} \sigma(Q_i) \right]^{1/m_Q}$$

Writing the exponent in equation (5):

$$\chi^2 = \sum_{i=1}^{m_Q} \frac{[S^C(Q_i) - S^E(Q_i)]^2}{\sigma^2(Q_i)} \quad (6)$$

we have  $P \propto \exp(-\chi^2/2)$  and it is immediately obvious that  $\chi^2/2$  in RMC plays the role of  $U/k_B T$  in the Metropolis Monte Carlo methodology.

The most important feature of this method is its independence from an interatomic potential, unlike standard atomistic modelling techniques. In this case the simulation is completely driven by the quality of the fit of the scattering calculated from the model to the experimental data. From the initial configuration the  $\chi_0^2$  between model and experimental  $S(Q)$  is evaluated. The structure is then modified by a random move of one atom. This move is subject both to constraints imposed on the coordination number and the bond length of each atom type and to the requirements of a fixed density and an excluded volume (the last condition being achieved through the assignment of closest distances of approach for all atom types). The model structure factor is recalculated and the new  $\chi_n^2$  is obtained. If  $\chi_n^2 < \chi_0^2$ , the

move is accepted. If  $\chi_n^2 > \chi_0^2$ , the move is accepted with probability  $\exp[-(\chi_n^2 - \chi_0^2)/2]$ , otherwise it is rejected. The procedure is repeated until  $\chi^2$  reaches an equilibrium value around which it oscillates.

Key ingredients of the procedure are the maximum allowed size of each random move  $d$  and the chosen standard deviation  $\sigma$ . The parameter  $d$  determines both the ratio of accepted to rejected moves and the amount of change in the structure with each move. For polymeric materials it is preferable to choose small move sizes, to ensure the preservation of chain connectivity and allow a reasonable number of moves to be accepted. This has the consequence of causing small structural changes, with the possibility of trapping some of the atoms in local arrangements. The problem is reduced if the starting configuration approximates a random structure, rather than, for instance, an ordered arrangement such as a crystalline one.

The standard deviation  $\sigma$  is also, to a certain extent, a parameter of the simulation. From the previous analogy  $\chi^2 = U/k_B T$ , it follows that  $\sigma = k_B T$ . Therefore  $\sigma$  is analogous to a temperature. A typical value for  $\sigma$  is the experimental error. However, if the simulation runs into a local minimum,  $\sigma$  can be increased and reduced again later on, once the structural configuration has moved away from this minimum.

RMC constitutes an attractive methodology for the production of structural models of disordered systems from diffraction data, due both to the lack of *a priori* assumptions on the interatomic potential for the system of interest and to the fact that all the available structural data are used in the simulation rather than just particular features. The quality of the structural configuration obtained is obviously dependent on the accuracy of the experimental data. It is also to be stressed that certainly the model to which the RMC calculation converges does not necessarily correspond to the unique, lowest energy configuration of the system of interest; it does, however, represent one possible structural picture, which is a realistic one in so far as it correctly predicts the experimentally measured properties of the material. In order to assess the energy characteristics of this model, we need expressions relating the various interactions, i.e. the force fields used in other atomistic approaches. We have deliberately excluded such input from the RMC approach so as to be able to compare directly structures which fit the experimental data with those produced from simulation using force fields that were derived from collated data. The RMC offers the possibility of effectively validating the force fields used in predictive atomistic modelling.

RMC was originally developed for the study of fluids and glassy systems and is not yet optimized for polymeric materials. In spite of this, the technique has proved extremely successful, as we will show, in the structural analysis of PE. Application to more complex polymers will certainly require tailoring of the RMC computational procedures to the realm of macromolecules.

#### CONVENTIONAL ATOMISTIC MODELLING TECHNIQUE

Our second approach to the data interpretation has followed an entirely different and independent route, based on conventional atomistic methods. We made use

of the CHARMM modelling package, from Harvard University, running on the same Silicon Graphics workstation that was employed in the RMC calculations.

Usually the structure generated by the amorphous growth procedure described above is, as mentioned earlier, in a high energy state. We therefore relaxed such a structure to a more realistic conformation. We achieved this by first performing a molecular mechanics minimization on it. This was done by using the CHARMM force field and minimization methods<sup>28</sup>. Subsequently, to avoid having a system trapped in a metastable high energy local minimum, we submitted it to a short CHARMM constant volume molecular dynamics (MD) run<sup>28</sup>. The run was composed of the three typical steps of heating to the temperature at which the experiment was performed, equilibration at that temperature and, finally, production. Each step lasted 5 ps. The time step was 0.001 ps. A monitor of the temperature and energy profile during the run permitted the evolution of the MD simulation to be followed and the achievement of equilibrium to be confirmed, as will be discussed in the next section.

#### PRESENTATION OF RESULTS AND DISCUSSION

Figure 1 shows the experimental structure factor  $S(Q)$  obtained for PE at  $T = 145^\circ\text{C}$ , after data reduction and conversion of the scattering function units to those of a coherent scattering intensity per atom. This result is in good agreement with the data reported in the literature<sup>9</sup>. The scattering pattern below  $2 \text{ \AA}^{-1}$  is determined by interchain correlations, whereas intrachain interactions are reflected in the remaining portion of the  $S(Q)$  spectrum<sup>3</sup>. The availability of reliable data up to  $35 \text{ \AA}^{-1}$ , due to the pulsed character of the ISIS neutron beam, allows an accurate determination of the geometric parameters characterizing the chain, such as bond lengths and valence angles, and of the single chain preferential conformation. We have previously developed a detailed quantitative analysis methodology that extracts single chain properties from diffraction data taken over a wide  $Q$  range. We have applied this procedure to the case

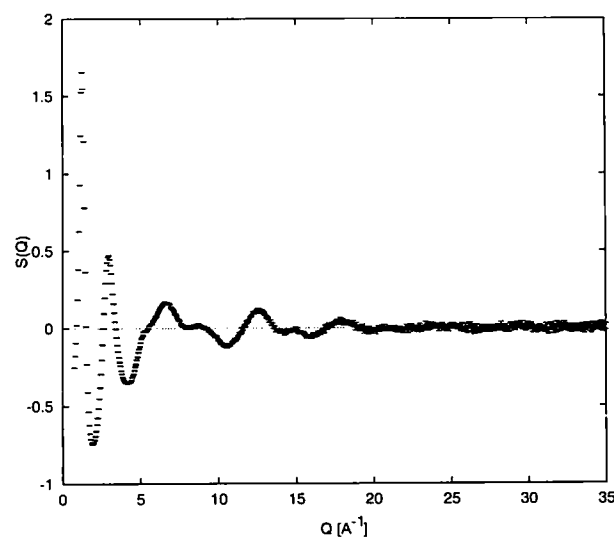


Figure 1 Experimental static structure factor  $S(Q)$  of deuterated PE at  $T = 145^\circ\text{C}$ , as a function of exchanged momentum  $Q$ , after data normalization and reduction. Experimental error bars are shown

of poly(tetrafluoroethylene)<sup>29</sup> and we have shown its accuracy. We are currently working on the application of this single chain technique to the data of Figure 1 (an alternative approach to the analysis of the high- $Q$  portion of the PE neutron diffraction pattern is given in ref. 9).

The amorphous growth procedure was performed with different choices of parameters to yield PE chains characterized by varying conformations, as mentioned earlier. The resulting chain topologies were extremely different one from the other, ranging from chains characterized by completely coiled and randomly arranged segments (fraction of *trans* torsions = 0.3) to straight and almost parallel segments (fraction of *trans* torsions = 0.9). This ensured that the starting models represented widely spaced points in the possible configurational space.

In correspondence of each type of topology, generated using different statistical weights for the rotational states, five similar structures were generated and the structure factor averaged over these five configurations.

The structures were then relaxed with the minimization procedures described above. Figure 2a shows the energy profile of a typical MD run. As can be seen, the total energy, increasing during the heating phase, slowly varies to finally settle, at the latest stages of the simulation, around a constant value, indicating that the structure has equilibrated. The process of structural relaxation was closely monitored by saving the model's atomic coordinates at regular time intervals and by evaluating, at

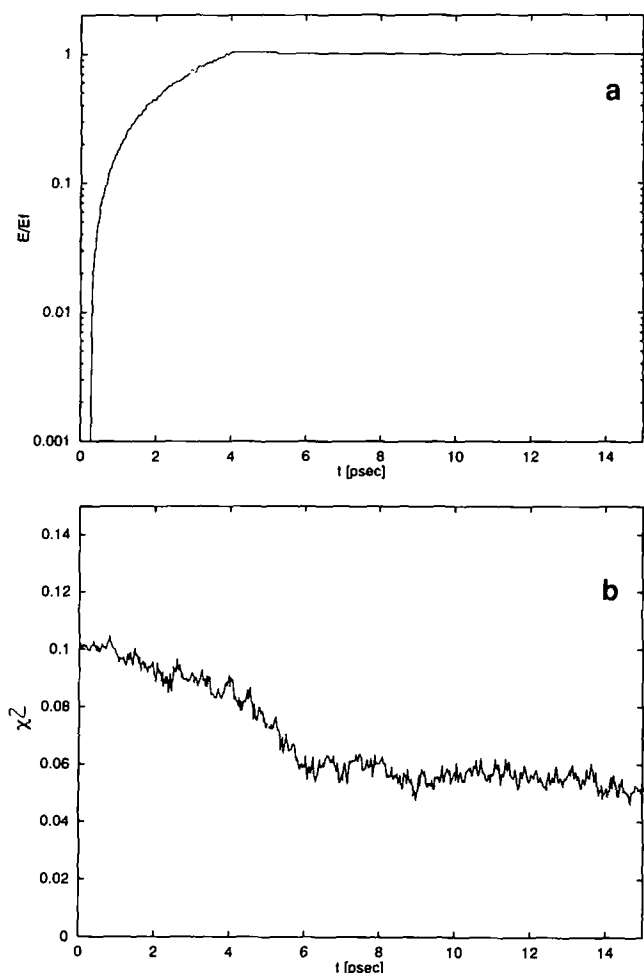


Figure 2 Analysis of a typical MD run: energy profile (a) and  $\chi^2$  (b) as functions of MD simulation time. The energies in (a), on a logarithmic scale, are normalized for the average final energy  $E_f$

each intermediate configuration, the deviation of the expected structure factor from the experimental  $S(Q)$  in terms of the  $\chi^2$  parameter defined in equation (6). Figure 2b shows the behaviour of  $\chi^2$  as a function of simulation time during the MD run. As can be seen, equilibrium is reached also from a structural point of view, although the  $\chi^2$  behaviour shows that the process of structural relaxation towards equilibrium is slower than that indicated by the energy evolution of the system.

Figures 3, 4 and 5 show the predicted behaviour of  $S(Q)$  from one of the atomistic models that were produced, at the three main generation stages discussed above, i.e. initial amorphous growth (Figure 3), molecular mechanics minimization (Figure 4) and MD run (Figure 5). This particular model corresponded to an initially rather coiled structure, with a fraction of the *trans* conformers of 0.34.

As can be seen, the starting model does not represent the experimental results very well (Figure 3). The peaks in the intrachain correlations region ( $Q > 2.0 \text{ \AA}^{-1}$ ) are qualitatively reproduced, but their shape and intensity are rather misrepresented; as to the first, the interchain peak that appears as a dominant feature in the

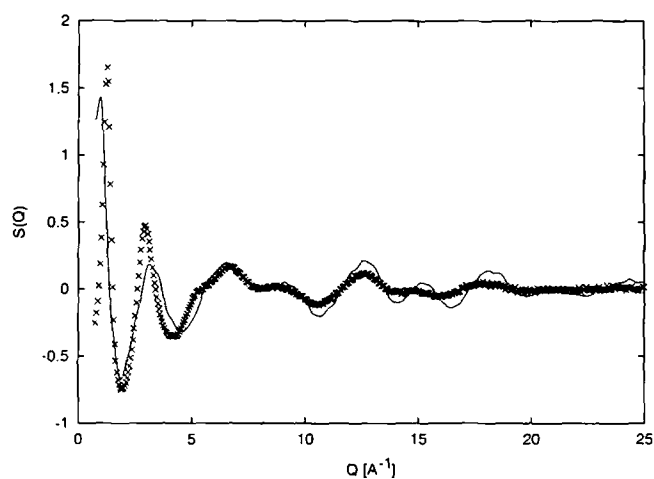


Figure 3 Typical model prediction of the structure factor  $S(Q)$  characterizing a PE structure generated by amorphous growth in a cubic box (solid line). Symbols are neutron scattering experimental results, shown for comparison

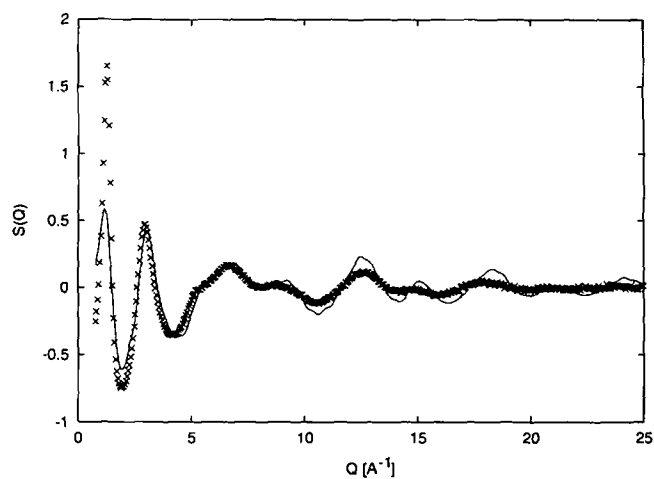


Figure 4 Model prediction of  $S(Q)$  after CHARMM minimization of the model structure of Figure 3. Key as in Figure 3

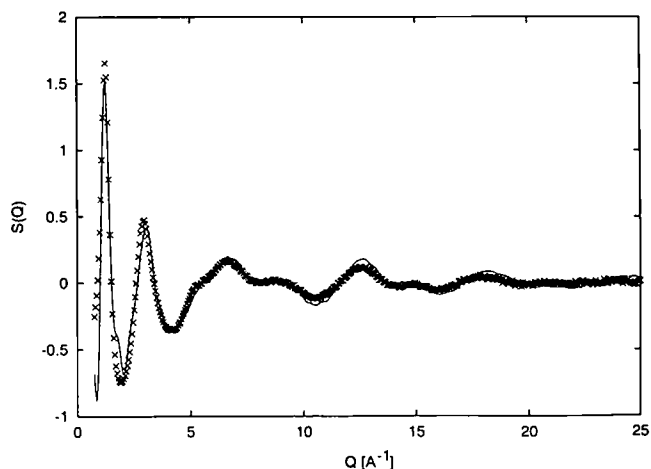


Figure 5 Model prediction of  $S(Q)$  after MD simulation of the model structure of Figure 4. Key as in Figure 3

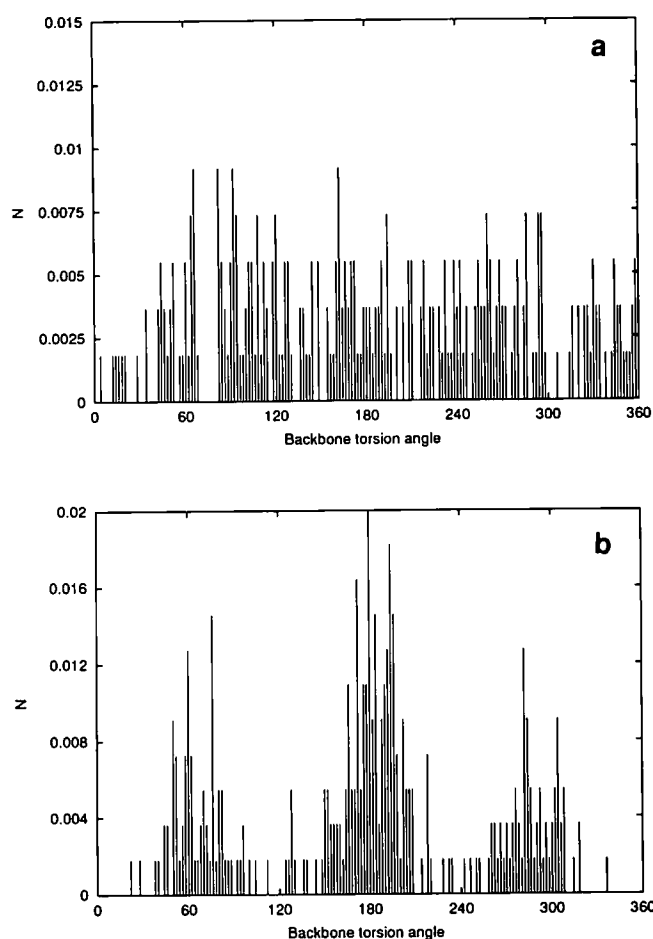


Figure 6 Distribution of backbone torsional angles for model structure after (a) initial amorphous growth and (b) MD run

experimental pattern, is completely absent in the model, indicating a gross distortion of chain packing effects.

As the model structure is relaxed with the techniques described earlier and the temperature of the specimen is taken into consideration, the predicted structure factor approaches the experimental results (Figures 4 and 5). It is to be noted that structures corresponding to very different initial conformations, due to different choices of ingredients in the amorphous growth, tend to configura-

tions with essentially the same structural characteristics once the specimen is subjected to these relaxation procedures. This is indicated not only by the fact that the model structure factors reproduce equally well the experimental data, but also by the close similarity of the model chains when examined in terms of the distributions of bond lengths, valence angles and torsional angles.

Figure 6 shows the distribution of torsional angles for the model at the end of the amorphous growth (Figure 6a) and after the MD run (Figure 6b). The corresponding structure factors are the ones shown in Figures 3 and 5, respectively. As can be seen, the model evolves from a very coiled chain to a more uncoiled one, characterized by a *trans* state and two *gauche* states, at  $\pm 120^\circ$ , with a fraction of *trans* torsion equal to 0.67. These results are comparable to the ones deduced from previous X-ray<sup>3,7,8</sup> and neutron diffraction<sup>9</sup> studies.

We have also analysed the orientational correlations between chain segments. The orientational order parameter has been calculated as sketched in Figure 7. Chain segments ( $i$  and  $j$  in Figure 7) are identified by three backbone atoms. 'Directors' are then associated to each segment and the distance  $r_{ij}$  between each pair of chain segments is calculated. The orientational order parameter  $f(r)$ , averaged over all chain segments, is finally evaluated:

$$f(r) = \left\langle \frac{3 \cos^2 \alpha_{ij}^r - 1}{2} \right\rangle_{ij}$$

Figure 8 shows a plot of  $f(r)$  as a function of  $r$ . In Figure 8a we represent the behaviour of the orientational correlations for the initial growth structure; Figure 8b shows the final result after the MD run. The most prominent features of these curves, i.e. the first three narrow peaks, merely represent intrachain correlations arising from regularities within the chain; as such, they are of no particular relevance in the present work. Interchain orientational correlations are expected to give rise to broad peaks. As can be seen, the initial model (Figure 8a) does not present any such orientational correlations. However, the model that correctly predicts the structure factor corresponds to a structure endowed with a certain degree of short range orientational correlation on a distance scale of about 4 Å (the broad

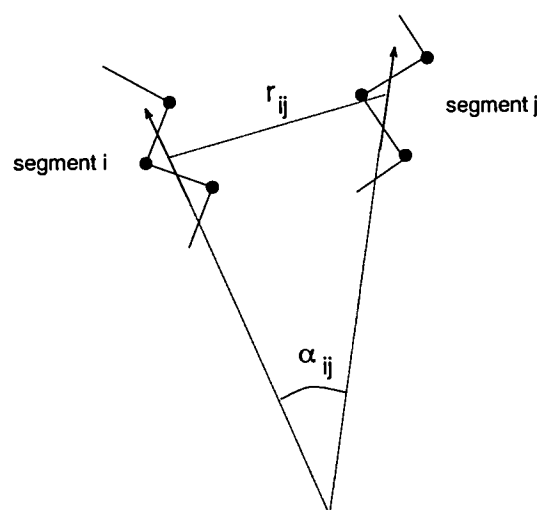


Figure 7 Schematic representation of the method utilized to evaluate chain orientational correlations

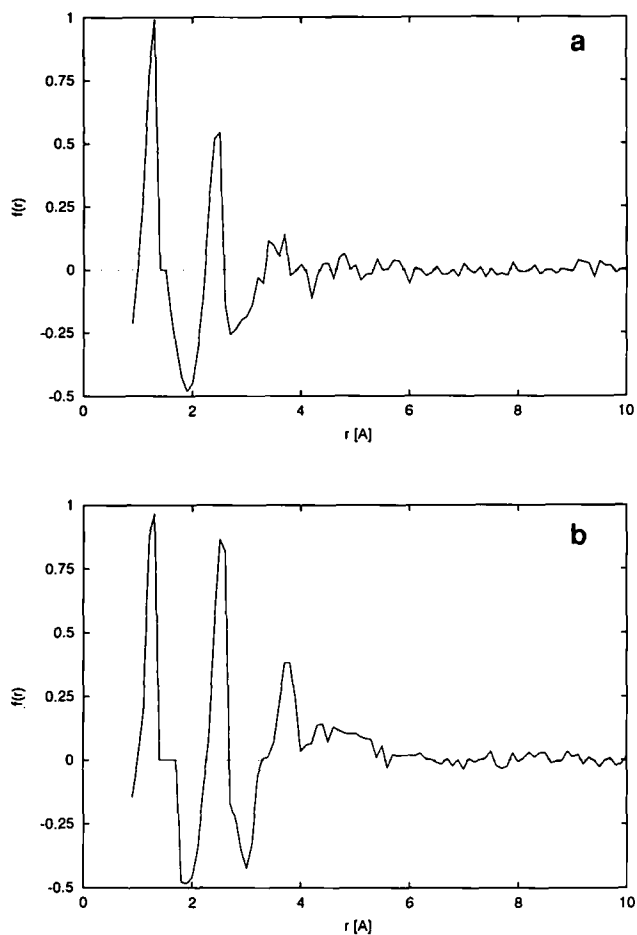


Figure 8 Orientational correlation function  $f(r)$  as a function of distance  $r$  for model structure after (a) initial amorphous growth and (b) MD run

peak of Figure 8b). This result is in agreement with earlier X-ray investigations<sup>3,30</sup> and model predictions<sup>31,32</sup>, although recently reported diffraction experiments have not been able to either give indications for it or rule it out<sup>7</sup>. This level of orientational correlations may be thought of as arising from an excluded volume effect around the near-neighbour chain segments.

The model chain initially obtained from the amorphous growth (whose structure factor is represented in Figure 3) was used as the starting structure for the RMC procedure. Constraints on the C-C and C-H bond length as well as on the C and H coordination numbers were imposed. The closest distances of approach for the two atom types were chosen as about 90% of their known distance. The correctness of these values was checked by ensuring that the calculated radial distribution functions did not present either sharp cutoffs or spikes in the low  $r$  region. A standard deviation  $\sigma$  of 1%, close to the estimated experimental error, was chosen.

The  $\chi^2$  minimization was performed on a 700 points dataset over the  $Q$  range  $0.5\text{--}35 \text{ \AA}^{-1}$ . The calculated  $\chi^2$  was constantly monitored; both the coordinates of the model and the corresponding structure factor were saved periodically in order to test the progress of the calculation.  $\chi^2$  decreased till it reached a saturation value after about  $3 \times 10^7$  total moves. The fraction of accepted moves was found to be 4%. The stability of  $\chi^2$  was at this point verified by letting the calculation proceed for

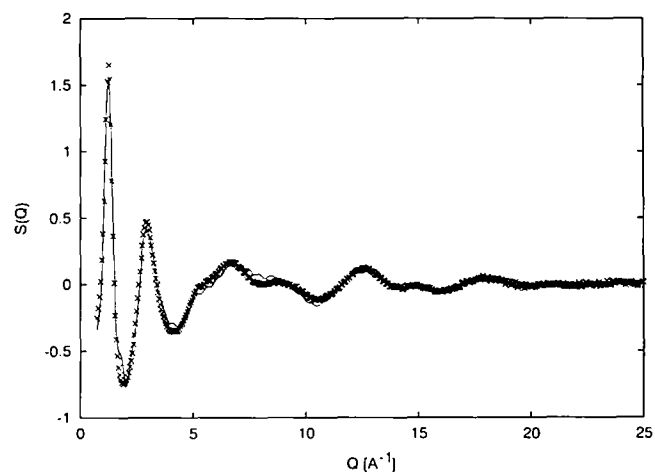


Figure 9 RMC fit (solid line) to the experimental  $S(Q)$  data (symbols). The fit was carried out up to  $35 \text{ \AA}^{-1}$

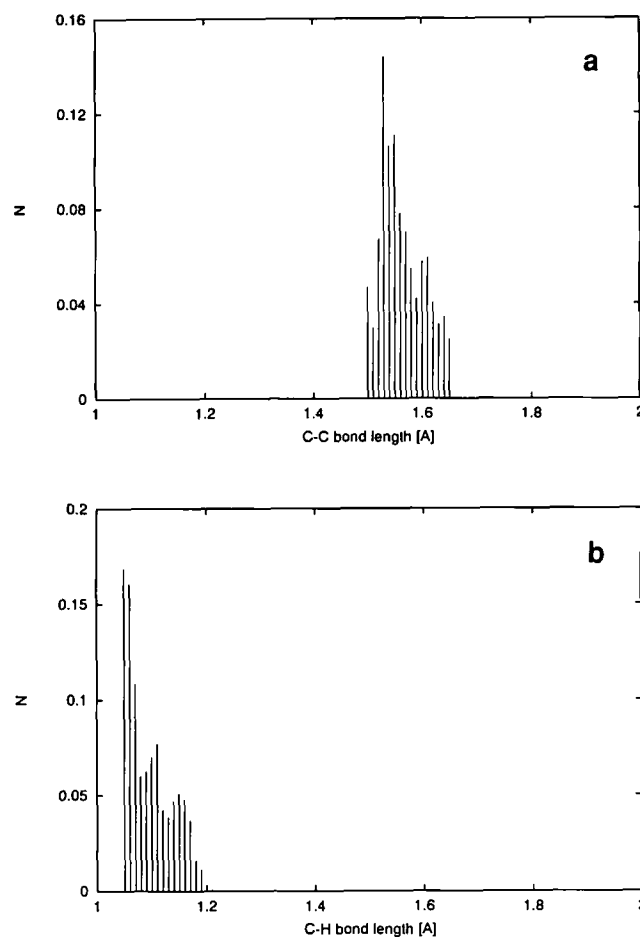
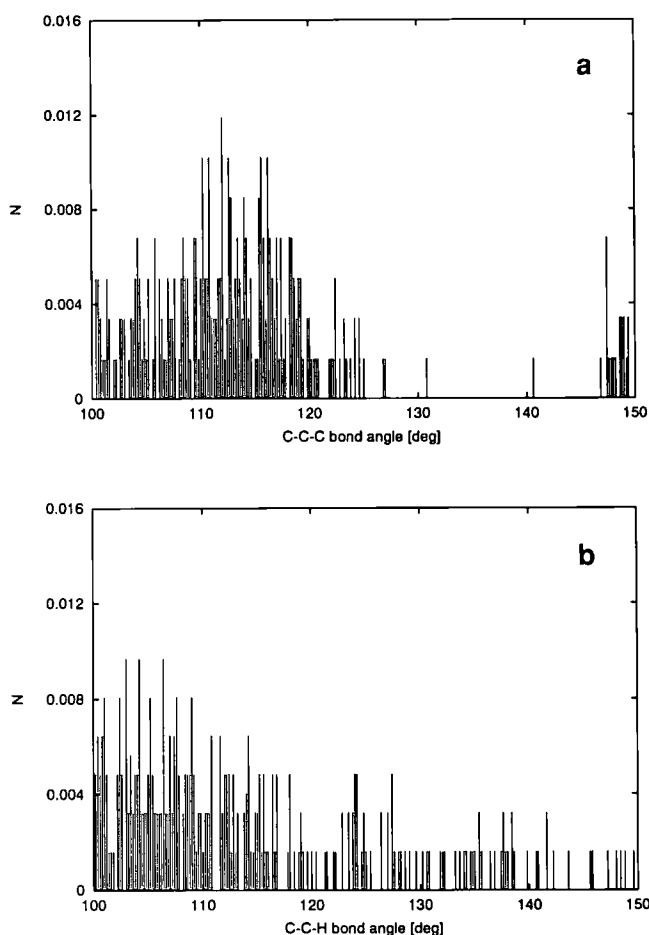
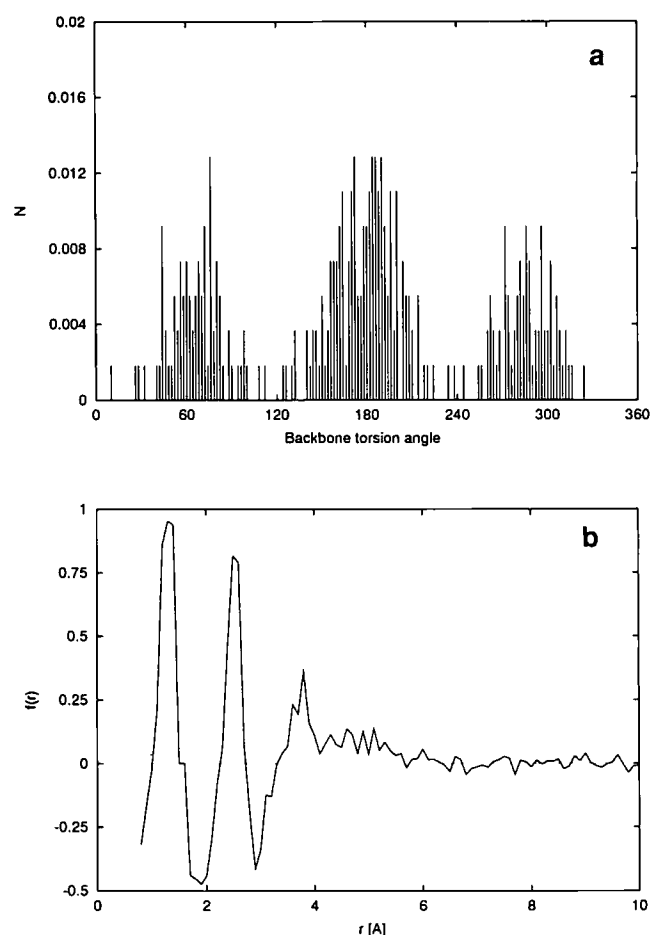


Figure 10 Features of the model structure resulting from the RMC fitting procedure: (a) C-C bond length distribution and (b) C-H bond length distribution

a further  $6 \times 10^6$  moves. At this point the calculation was terminated. Figure 9 shows the structure factor of the resulting model and its comparison with the experimental data. The fit is remarkably good over the whole  $Q$  range explored, as is inherent in the procedure. An analysis of the model structure in terms of distribution of bond lengths, valence angles, torsional angles and orientational correlations between chain segments, analogous to the



**Figure 11** Features of the model structure resulting from the RMC fitting procedure: (a) C-C-C valence angle distribution and (b) C-C-H valence angle distribution



**Figure 12** Features of the model structure resulting from the RMC fitting procedure: (a) distribution of backbone torsional angles and (b) orientational correlation function  $f(r)$  versus distance  $r$

one performed on the atomistic model, revealed a local arrangement of the chain completely similar to the one obtained from the alternative atomistic route, after the MD simulation. Figures 10, 11 and 12 show the results of this analysis. The C-C (Figure 10a) and C-H (Figure 10b) bond length distributions, as well as the C-C-C (Figure 11a) and C-C-H (Figure 11b) valence angle distributions, are acceptably narrow and can be considered representative of a macromolecular chain. As a comparison, Figure 13 shows the two valence angle distributions for the chain generated by the atomistic model of Figure 5. While the distribution of C-C-H bond angles generated by RMC (Figure 11b) is somewhat broader than the one expected and indeed predicted by atomistic modelling (Figure 13b), the backbone valence angles resulting from the RMC structure are characterized by a clearly more realistic distribution of values (Figure 11a) than the one generated by the MD simulation (Figure 13a).

The backbone torsional angle distribution (Figure 12a) and the orientational correlations between chain segments (Figure 12b) are strikingly similar to the ones shown in Figures 6b and 8b, indicating a somewhat unexpected convergence of the models from the two independent techniques. This is a remarkable result if, as previously mentioned, it is considered that there are no ingredients to the RMC recipe apart from simple geometric parameter

constraints that have the only scope of preventing the input structure evolving towards extremely unrealistic configurations.

In the amorphous growth/MD modelling procedure it is necessary to define a theoretical force field to be used in the simulation; the simulation itself can be regarded as a process of relaxation of the chain configuration towards a stable and low energy condition, always within the limits imposed by the force field itself. As far as the modelling procedure is concerned, the outcome will be in itself correct, if the structure has been given the opportunity to properly evolve towards an equilibrium condition. However, the comparison with experimental data is fundamental in establishing whether this resulting structure is not only correct but also realistic. An atomistic model that predicts the correct experimental results and that displays reasonable conformational properties for the system under investigation can be considered an acceptable representation of reality. Since the model for PE generated by our MD simulation follows these lines, as we have shown, we are confident that the procedure we utilized and the force field we chose are appropriate in realistically describing the very local structure of this polymer. This is not necessarily true for other macromolecules: since the expressions for the existing force fields are normally parameterized using small-molecule data, the only way to establish the validity



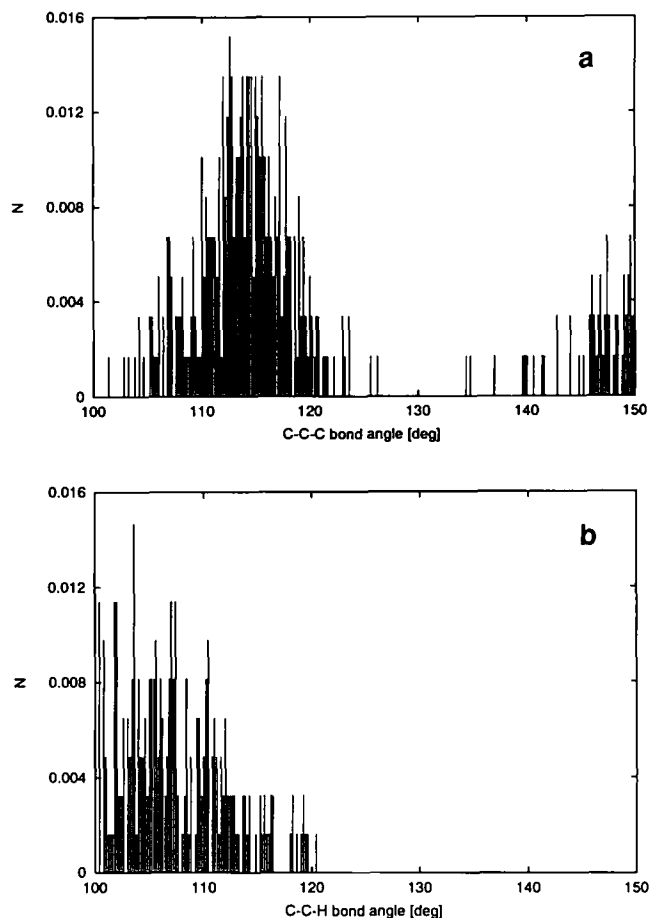


Figure 13 Features of the model structure resulting from the MD simulation (Figure 5): (a) C-C-C valence angle distribution and (b) C-C-H valence angle distribution

of any given potential for a particular polymer system is a close coupling between modelling procedure and experiment.

With RMC, however, there is no theoretical *a priori* input in the procedure. All the information needed to build a realistic picture of the system of interest is obtained from its diffraction pattern. The structural configuration to which RMC converges represents a chain conformation and, implicitly, a force field which were unknown at the beginning of the process and which have been directly extracted from experimental diffraction data. Whilst this does not ensure uniqueness of the obtained model, it certainly guarantees its reliability. We are currently exploring the possibility of an explicit determination of appropriate force field parameters by fits of the bond lengths and bond angle distributions obtained by the RMC procedure. Although the analytical form of the force field would be chosen *a priori*, the force field parameters thus extracted would be experimental in nature.

Despite the lack of optimization of the RMC approach to the study of polymeric samples, our results indicate clearly, we believe, the potential and power that this analysis route can have for a microscopic understanding of polymeric materials.

## CONCLUSIONS

In this preliminary investigation we have shown the

potential of the RMC procedure coupled with 'wide angle' diffraction experiments in the prediction of accurate bulk models of amorphous polymers. The model obtained for molten PE is reliable insofar as it accurately represents the experimental neutron diffraction results over the whole spatial region explored. The model polymer has the expected single chain properties and furthermore shows for the first time the onset of minimal orientational correlations on the basis of experimental data. This is achieved with a relatively inexpensive investment of computer time.

On the other hand, the success of the conventional atomistic modelling route in producing a model structure that converges, in its properties, with the one obtained by RMC confirms the reliability of RMC, besides showing the usefulness of molecular mechanics and molecular dynamics in the prediction of short range orientational correlations in amorphous polymers.

We believe that the success of the RMC procedure shown in this work constitutes a step forward in the establishment of quantitatively accurate data analysis techniques for the investigation of the local structure in amorphous polymers, at least for simple materials such as PE.

We are currently exploring the optimization of RMC to the study of macromolecules and the extension of the described analysis strategies to more complex and more interesting polymeric materials.

## ACKNOWLEDGEMENTS

This work forms part of the Courtauld's Polymer Science Prize Programme at the University of Reading. It was also supported by the Science and Engineering Research Council. We acknowledge Polygen (now Molecular Simulations Inc.) for support, Dr Robert McGreevy and Dr Malcolm Howe (Clarendon Laboratory, Oxford, UK) for their provision of the RMC program and Dr Alan Soper (ISIS, Chilton, UK) for his help with the SANDALS experiments.

## REFERENCES

- Mitchell, G. R. in 'Order in the Amorphous "State" of Polymers' (Eds S. E. Keinath, R. L. Miller and J. K. Rieke), Plenum Press, New York, 1987, p. 1
- Mitchell, G. R. in 'Comprehensive Polymer Science' (Eds G. Allen, J. C. Bevington, C. Booth and C. Price), Pergamon Press, Oxford, 1989, Vol. I, Ch. 31, p. 687
- Mitchell, G. R., Lovell, R. and Windle, A. H. *Polymer* 1982, **23**, 1273
- Schelten, J., Ballard, D. G. H., Wignall, G. D., Longman, G. and Schmatz, W. *Polymer* 1976, **17**, 751
- Schelten, J., Wignall, G. D., Ballard, D. G. H. and Longman, G. W. *Polymer* 1977, **18**, 1111
- Flory, P. J. 'Statistical Mechanics of Chain Molecules', Wiley, New York, 1969
- Narten, A. H. *J. Chem. Phys.* 1989, **90**, 5857
- Narten, A. H., Habenschuss, A., Honnell, K. G., McCoy, J. D., Curro, J. G. and Schweizer, K. S. *J. Chem. Soc. Faraday Trans.* 1992, **88**, 1791
- Misawa, M., Kanaya, T. and Fukunaga, T. *J. Chem. Phys.* 1991, **94**, 8413
- Schweizer, K. S. and Curro, J. G. *Phys. Rev. Lett.* 1987, **58**, 246
- Curro, J. G. and Schweizer, K. S. *J. Chem. Phys.* 1987, **87**, 1842
- Honnell, K. G., McCoy, J. D., Curro, J. G., Schweizer, K. S., Narten, A. H. and Habenschuss, A. *J. Chem. Phys.* 1991, **94**, 4659
- Flory, P. J. *J. Chem. Phys.* 1949, **17**, 303

*Atomistic model of molten polyethylene: B. Rosi-Schwartz and G. R. Mitchell*

- 14 Binder, K. and Heermann, D. W. 'Monte Carlo Simulation in Statistical Physics: An Introduction', Springer, Berlin, 1988
- 15 Kremer, K. and Binder, K. *Comput. Phys. Rep.* 1988, **7**, 259
- 16 Ciccotti, G. and Hoover, W. G. 'Molecular Dynamics Simulations of Statistical Mechanical Systems', North-Holland, Amsterdam, 1986
- 17 Kremer, K. and Grest, G. S. *J. Chem. Phys.* 1990, **92**, 5057
- 18 Baschnagel, J., Binder, K., Paul, W., Laso, M., Suter, U. W., Batoulis, I., Jilge, W. and Bürger, T. *J. Chem. Phys.* 1991, **95**, 6014
- 19 Baschnagel, J., Qin, K., Paul, W. and Binder, K. *Macromolecules* 1992, **25**, 3117
- 20 de Pablo, J. J., Laso, M. and Suter, U. W. *J. Chem. Phys.* 1992, **96**, 2395
- 21 Soper, A. K. in 'Proceedings of ICANS X, Los Alamos, 1988' (Ed. D. K. Hyer), IOP Conference Series no. 97, 1989
- 22 Rosi-Schwartz, B., Mitchell, G. R. and Soper, A. K. *Polymer* 1992, **33**, 3744
- 23 Howells, W. S., Soper, A. K. and Hannon, A. C. Technical Report RAL-89-046, Rutherford Appleton Laboratory, Chilton, Oxfordshire, UK, 1989
- 24 Cun Feng Fan and Shaw Ling Hsu. *Macromolecules* 1991, **24**, 6244
- 25 Cun Feng Fan and Shaw Ling Hsu. *Macromolecules* 1992, **25**, 266
- 26 McGreevy, R. L. and Pustzai, L. *Mol. Simulation* 1988, **1**, 359
- 27 McGreevy, R. L., Howe, M. A., Keen, D. A. and Clausen, K. N. Technical Report OUCL 90/03, Clarendon Laboratory, University of Oxford, 1990
- 28 'Molecular Simulations', CHARMM User Guide, Molecular Simulations Inc., Burlington, MA, USA, 1988
- 29 Rosi-Schwartz, B. and Mitchell, G. R. *Polymer* 1994, **35**, 3139
- 30 Mitchell, G. R., Lovell, R. and Windle, A. H. *Polymer* 1980, **21**, 989
- 31 Aitken, D., Glotin, M., Hendra, P. J., Jabic, H. and Marsden, E. *J. Polym. Sci. B*, 1976, **14**, 619
- 32 Pechołd, W. *Makromol. Chem. Suppl.* 1984, **6**, 163